available at www.sciencedirect.com

ScienceDirect

journal homepage: www.elsevier.com/locate/chnjc

Chinese Journal of Catalysis
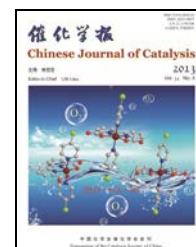
Article

Immobilization of highly active Pd nano-catalysts on functionalized mesoporous silica supports using mercapto groups as anchoring sites and their catalytic performance for phenol hydrogenation

Jiaxi Zhang [a], Gaowei Huang [a], Cheng Zhang [a,b], Qunhua He [b], Chao Huang [a], Xu Yang [c], Huiyu Song [a], Zhenxing Liang [a], Li Du [a,d,*], Shijun Liao [a,d,#]

[a] School of Chemistry and Chemical Engineering, South China University of Technology, Guangzhou 510640, Guangdong, China
[b] Guangdong Environmental Monitoring Center, Guangzhou 510640, Guangdong, China
[c] Key Laboratory of Renewable Energy and Gas Hydrate, Guangzhou Institute of Energy Conversion, Chinese Academy of Sciences, Guangzhou 510640, Guangdong, China
[d] The Key Laboratory of Fuel Cell Technology of Guangdong Province, School of Chemistry and Chemical Engineering, South China University of Technology, Guangzhou 510640, Guangdong, China

ARTICLE INFO

ABSTRACT

Highly active and highly dispersed Pd-loaded nano-catalysts using mercapto group (–SH) functionalized mesoporous silica supports, namely, Pd-SH-MCM-41 and Pd-SH-SBA-15, were prepared using an impregnation-reduction approach. The surface –SH groups are believed to facilitate the high distribution and immobilization of the Pd nanoparticles within the silica supports through an anchoring interaction. The catalysts featured long-range ordered structures, uniform pore size, high surface area, and highly dispersed Pd nanoparticles as characterized by X-ray diffraction, N_2 adsorption-desorption, and transmission electron microscopy. The catalysts showed activity five times higher than that of commercial Pd/C catalyst and three times higher than those of Pd/MCM-41 and Pd/SBA-15 catalysts. Within 1 h of reaction at 80 °C and 1.0 MPa, the conversion of phenol attained was greater than 99%, and the selectivity for cyclohexanone was 98%.

1. Introduction

Mesoporous silicas are important functional nanomaterials with unique properties. Because of their properties, such as uniform pore structures, adjustable pore size, large pore volume, high surface area, and modifiable functional groups on the surface, they have attracted increasing attention in multiple areas including catalysis, adsorption, separation, sensors, and drug delivery. Over the years, both synthesis and catalysis have become popular areas of research [1,2].

Catalytic hydrogenation of phenol to cyclohexanone is of commercial and environmental significance because cyclohexanone is an important intermediate for the manufacture of dyestuffs and pharmaceutical products; it is also a key raw ma-

terial for producing caprolactam for Nylon 6 and adipic acid for Nylon 66 [3]. Therefore, selective hydrogenation of phenol to cyclohexanone is an important chemical process that has been extensively studied to date [4–9]. A broad range of catalysts, such as Raney Ni [4], Pd-based films [5], amorphous alloys [6], bimetal catalysts [7], and supported catalysts [8, 9], have been developed for this purpose. However, issues relating to relatively low catalytic efficiencies and the need for severe reaction conditions (>150 °C in the vapor phase [10] or >10 MPa in sc-CO_2 medium [11,12]) have limited the practical application of such catalysts. Recently, Liu et al. [13] demonstrated the potential of using a dual supported Pd-Lewis acid catalyst for the hydrogenation of phenol under mild conditions (50 °C, 1.0 MPa), achieving a complete phenol conversion with the selectivity to cyclohexanone of >99.9%.

Based on our preliminary work on the hydrogenation of phenol using noble metal-loaded mesoporous silica materials as catalysts [14], we designed a new method to prepare highly dispersed Pd-loaded nano-catalysts. Mercapto groups (–SH) were first grafted onto the mesoporous silica supports, MCM-41 and SBA-15. The supports were then loaded with highly active Pd nanoparticles with –SH serving as anchor points. The Pd-loaded nano-catalysts were then assessed for the hydrogenation of phenol under mild conditions.

2. Experimental

2.1. Catalyst preparation

2.1.1. Preparation of MCM-41 support nanoparticles

Cetyltrimethylammonium bromide (CTAB, Aldrich, 1.0 g) as a template was dissolved in 480 ml H_2O and 3.5 ml NaOH (2 mol/L) solution with stirring at 80 °C for 1 h. After dissolution was complete, tetraethyl orthosilicate (TEOS, Tianjin Kemiou, 4.5 ml) was added dropwise and the mixture was stirred at 80 °C for 2 h. The final product was recovered by filtration, dried under vacuum, and calcined at 550 °C in air for 6 h to obtain the white MCM-41 powder.

2.1.2. Preparation of SBA-15 support nanoparticles

Triblock copolymer $EO_{20}PO_{70}EO_{20}$ (P123, M_w = 5800, Aldrich, 4.0 g) was dissolved in 126 ml H_2O and 20 ml HCl (37%) solution, and the mixture was stirred at 35 °C for 2 h. TEOS (9.2 ml) was then added to the solution and hydrolyzed at 35 °C for 20 h under vigorous stirring. The mixture was transferred into a sealed Teflon-lined vessel and heated at 100 °C for 12 h. The resulting solid was filtered and washed, dried under vacuum, and calcined at 550 °C in air for 6 h to obtain the white SBA-15 powder.

2.1.3. Preparation of –SH-functionalized support nanoparticles

MCM-41 or SBA-15 mesoporous silica nanoparticles (100 mg) were immersed in 10 ml toluene solution containing (3-mercaptopropyl)trimethoxysilane (Gelest, 100 μl) and heated under reflux at 80 °C for 24 h. The nanoparticles were recovered by filtration, washed thoroughly with ethanol, and dried in a vacuum oven. The –SH-functionalized nanoparticles

are denoted SH-MCM-41 and SH-SBA-15.

2.1.4. Preparation of Pd-SH-MCM-41 and Pd-SH-SBA-15 catalysts

The Pd-loaded catalysts were prepared by an impregnation-hydrogen reduction process. SH-MCM-41 or SH-SBA-15 (1.0 g) was carefully dispersed in a solution containing 0.0833 g $PdCl_2$, 2 ml HCl (37%), and 3 ml H_2O. After impregnation for 24 h, the particles were filtered and thoroughly washed with water to obtain a clear filtrate. The particles were then dried overnight in a vacuum oven at 70 °C and heated in a tubular furnace at 200 °C under a H_2 reducing atmosphere (flow = 20 ml/min) for 2 h. The Pd-loaded –SH-functionalized silica catalysts are denoted Pd-SH-MCM-41 and Pd-SH-SBA-15. Pd-loaded nano-catalysts using non-functionalized MCM-41 and SBA-15 as supports were prepared and denoted Pd/MCM-41 and Pd/SBA-15, respectively.

2.2. Characterization of catalysts

X-ray diffraction (XRD) patterns were collected on a Shimadzu XD-3A X-ray diffractometer (Japan) using Cu K_α radiation (40 kV, 30 mA). N_2 adsorption-desorption isotherms were measured on a Micromeritics ASAP 2010 analyzer (USA). Prior to analysis, the samples were evacuated at 120 °C for 24 h. Fourier transform infrared (FT-IR) spectra were recorded on a Bruker TENSOR 27 FT-IR instrument (Germany) to confirm the presence of functional groups on the catalyst surface. Transmission electron microscopy (TEM) was carried out on a JEOL JEM-2010 microscope (Japan) using an accelerating voltage of 200 kV.

2.3. Evaluation of catalysts

The activity of the prepared catalysts was evaluated by the hydrogenation of phenol. The reaction was carried out in a stainless steel autoclave (50 ml) equipped with a magnetic stirrer and Teflon thermostat. The reaction mixture comprised 1.0 g phenol, 0.2 g catalyst, and 10 ml CH_2Cl_2 as solvent. Prior to reaction, the system was purged with pure H_2 (99.99%) thrice to remove air. The evaluation was conducted at 80 °C and 1.0 MPa of hydrogen pressure for 1 h. Following reaction, the solution containing the catalysts was centrifuged, and the supernatants were analyzed using gas chromatography-mass spectrometry (GCMS-QP2010SE, Japan) to identify cyclohexanone and cyclohexanol.

3. Results and discussion

3.1. Characterization of supports and catalysts

The mesostructures of the silica supports and Pd-loaded nano-catalysts were examined using small-angle XRD. As depicted in Fig. 1, both MCM-41 and SBA-15 supports exhibit one sharp diffraction peak from the (100) plane and two weak diffraction peaks corresponding to the (110) and (200) planes, respectively, indicating the presence of a long-range ordered
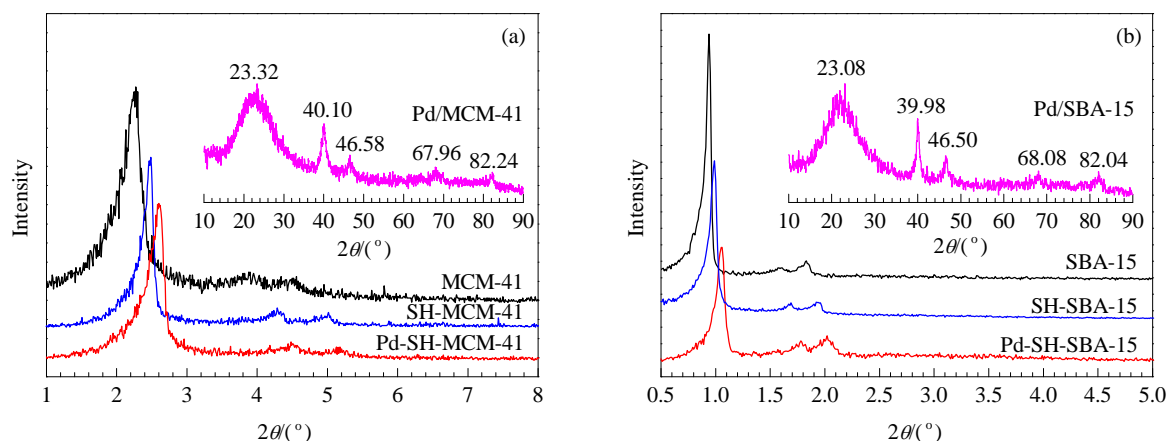
Fig. 1. XRD patterns of MCM-41 series (a) and SBA-15 series (b) samples.

structure. Relative to the diffraction peak ($2\theta = 2°$–$3°$) observed in the MCM-41 sample, both SH-MCM-41 and Pd-SH-MCM-41 samples display a slight shift toward the higher angle region (Fig. 1(a)), suggesting a reduced *d*-spacing value and smaller pore size as a result of –SH functionalization and Pd loading. As depicted in the wide-angle XRD pattern (Fig. 1(a), inset), the Pd-loaded catalyst (Pd/MCM-41) exhibits four diffraction peaks at 40.1°, 46.58°, 67.96°, and 82.24° corresponding to the (111), (200), (220), and (311) planes of the face-centered cubic structure of palladium, respectively, confirming metallic palladium loading on the support after hydrogen reduction. This sample also shows a diffraction peak at around 23°, which is

attributed to amorphous SiO_2 [15]. The broad peaks could be due to highly distributed Pd nanoparticles within the support, small particle size, or the amorphous structure of the sample. It should be pointed out that the Pd-SH-MCM-41 catalyst also exhibits comparable broad diffraction peaks, suggesting the formation of small Pd particles following binding of the Pd cations with the –SH anchor groups. The SBA-15 series samples displayed similar results to the MCM-41 series samples.

Figure 2 shows N_2 adsorption-desorption isotherms and pore size distributions for the prepared samples. MCM-41, SH-MCM-41, and Pd-SH-MCM-41 samples (displaying a pore size distribution centered at 2–3 nm) feature a type IV isotherm
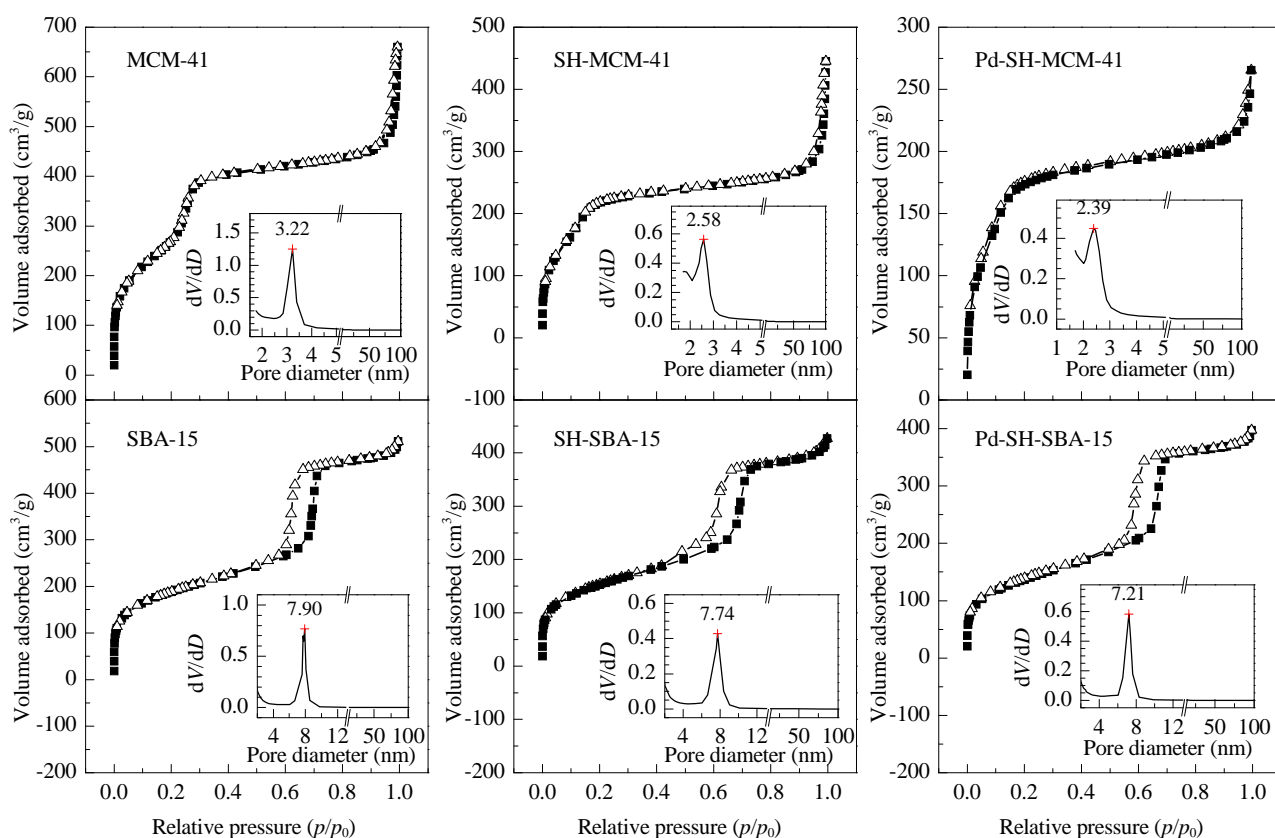

Fig. 2. N_2 adsorption-desorption isotherms and BJH pore size distribution of the mesoporous silica supports and catalysts.
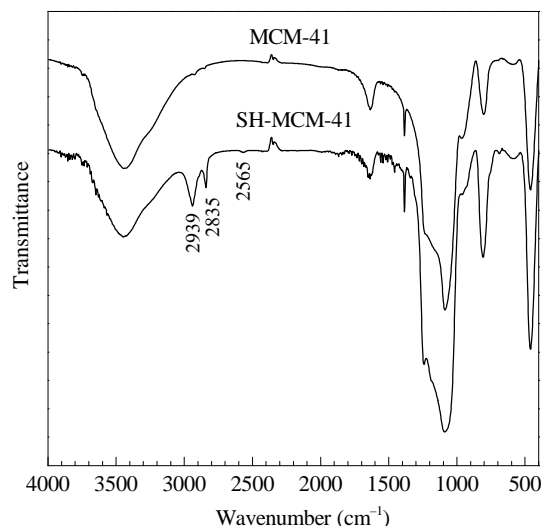
Table 1
Textural properties of the mesoporous silica supports and catalysts.

Sample	A_{BET} (m²/g)	BJH pore size (nm)	Pore volume (cm³/g)
MCM-41	1085	3.22	1.21
SH-MCM-41	740	2.58	0.86
Pd-SH-MCM-41	591	2.39	0.56
SBA-15	647	7.90	0.87
SH-SBA-15	526	7.74	0.74
Pd-SH-SBA-15	476	7.21	0.70

Fig. 3. FT-IR spectra of MCM-41 and SH-MCM-41 samples.

with no hysteresis loop, in agreement with the findings reported in Ref. [16]. Likewise, SBA-15, SH-SBA-15, and Pd-SH-SBA-15 samples exhibit a type IV isotherm. However, the isotherm feature a distinct H1 hysteresis loop at relative pressures of p/p_0 = 0.5–0.8 that can be associated with the presence of an ordered mesoporous structure [17,18]. The textural properties of the mesoporous silica supports and catalysts are listed in Table 1. The –SH-functionalized nanoparticles display surface areas as high as 740 m²/g (SH-MCM-41) and 526 m²/g (SH-SBA-15) that would be beneficial to achieving a high loading dispersion of Pd nanoparticles into the SH-MCM-41 or SH-SBA-15 support materials. Upon Pd loading, a decrease in surface area was noted for Pd-SH-MCM-41 and Pd-SH-SBA-15; however, the surface area values are much higher than that of commercial Pd/C catalysts (250 m²/g) [14]. A slight reduction in pore size was also obtained for the –SH-functionalized and Pd-loaded samples, but the highly uniform mesoporous structure and high surface area were retained.

FT-IR spectroscopy was used to verify the presence of grafted –SH groups onto the silica supports. Typical FT-IR spectra for the MCM-41 series samples are shown in Fig. 3. All samples show Si–O–Si bands at 1089, 797, and 468 cm⁻¹ [19].

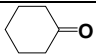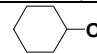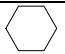Additional bands at 2939 and 2835 cm⁻¹ corresponding to C–H stretches [20] and at 2565 cm⁻¹ that can be attributed to a S–H stretch were observed in the SH-MCM-41 sample, confirming the successful grafting of –SH functional groups onto the MCM-41 support.

TEM analysis was conducted to examine the effect of –SH functionalization and Pd loading on the mesostructure of the support as well as to assess the degree of Pd nanoparticles dispersion within the support (Fig. 4). The typical MCM-41 mesopore structure is well maintained within the Pd-SH-MCM-41 sample that features particle sizes of ~100 nm (Fig. 4(a)). The well dispersed Pd nanoparticles (2–3 nm) within the silica support can be observed in the high-resolution TEM image (Fig. 4(b)). Importantly, no aggregated Pd nanoparticles were ob-
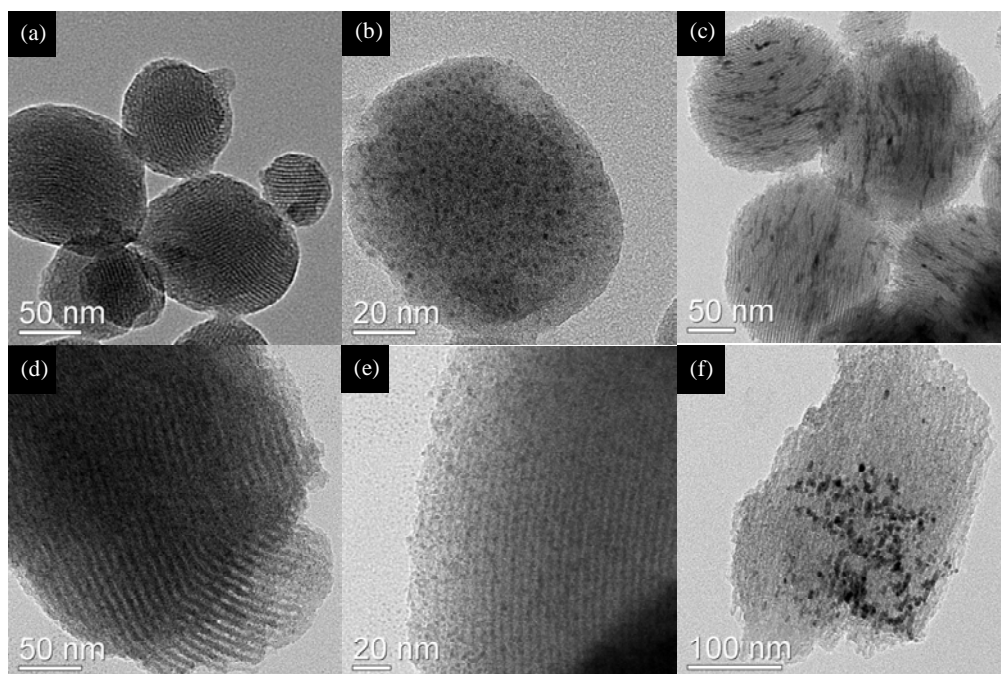
Fig. 4. TEM images of the Pd catalysts. (a, b) Pd-SH-MCM-41; (c) Pd/MCM-41; (d, e) Pd-SH-SBA-15; (f) Pd/SBA-15.

Table 2
Hydrogenation of phenol catalyzed by different catalysts.

Catalyst	Conversion (%)	Selectivity (%)		
		⬡=O	⬡–OH	⬡
MCM-41	—	—	—	—
SBA-15	—	—	—	—
Pd/C	16.9	83.4	11.7	4.9
Pd/MCM-41	32.2	87.1	8.3	4.6
Pd/SBA-15	31.8	82.6	9.7	7.7
Pd-SH-MCM-41*	>99	98.1	1.9	—
Pd-SH-SBA-15*	>99	97.8	2.2	—
Pd/MCM-41*	1.2	12.3	38.5	49.2
Pd/SBA-15*	0.9	10.2	24.7	65.1

Reaction conditions: phenol/Pd mass ratio = 1:0.01, 10 ml CH_2Cl_2, 80 °C, 1.0 MPa of H_2, stirring speed 1000 r/min. *The catalyst was thoroughly washed after impregnation until a clear filtrate was obtained.

served. In contrast, both Pd/MCM-41 (Fig. 4(c)) and Pd/SBA-15 (Fig. 4(f)) samples feature large and aggregated Pd nanoparticles. This observation was consistent with the XRD results. While –SH functionalization did not impact the mesopore structure of the silica supports (MCM-41 and SBA-15), the presence of –SH functional groups was crucial to producing highly dispersed Pd nano-catalysts.

3.2. Catalytic activity

Table 2 shows the performance of different catalysts for the hydrogenation of phenol. Both MCM-41 and SBA-15 exhibited minimal activity, whereas Pd/C achieved a conversion of 16.9%. Improved conversions were obtained for Pd/MCM-41 and Pd/SBA-15 (up to 32.2% and 31.8%, respectively). However, Pd-SH-MCM-41 and Pd-SH-SBA-15 catalysts achieved the highest conversion (>99%), with a high cyclohexanone selec-

tivity of 98.1% and 97.8%, respectively. These findings show that highly dispersed Pd nanoparticles significantly improve the performance of the catalyst. To assess the attachment of the Pd nanoparticles onto the silica surface via –SH anchor groups, the following tests were conducted. When MCM-41 and SBA-15 were used as supports, the color of the supernatant, following impregnation with the H_2PdCl_4 solution, remained orange. Furthermore, the color of the impregnated Pd/MCM-41 and Pd/SBA-15 particles became almost colorless following thorough washing, indicating that the active Pd component was washed away. In contrast, when SH-MCM-41 and SH-SBA-15 were used as supports, the resulting impregnated particles displayed a bright orange color and a colorless supernatant solution was obtained following washing. These results confirm that the Pd nanoparticles are strongly attached to the silica surface via –SH anchor groups.

4. Conclusions

Highly dispersed Pd-loaded nano-catalysts using –SH-functionalized mesoporous silica as supports were successfully synthesized. (3-Mercaptopropyl)trimethoxysilane was used as the –SH source. The –SH functional groups served as effective anchoring groups for the attachment of Pd nanoparticles onto the silica support. Our results showed that –SH functionalization and Pd loading processes did not affect the mesopore structure of the silica supports: the Pd-SH-MCM-41 and Pd-SH-SBA-15 nanoparticles displayed a well maintained mesopore structure with a uniform pore structure and high surface area. Both Pd-SH-MCM-41 and Pd-SH-SBA-15 catalysts displayed superior activity to commercial Pd/C catalyst (five times higher) and Pd/MCM-41 and Pd-SBA-15 catalysts (three times higher).

Graphical Abstract

Immobilization of highly active Pd nano-catalysts on functionalized mesoporous silica supports using mercapto groups as anchoring sites and their catalytic performance for phenol hydrogenation

Jiaxi Zhang, Gaowei Huang, Cheng Zhang, Qunhua He, Chao Huang, Xu Yang, Huiyu Song, Zhenxing Liang, Li Du *, Shijun Liao *
South China University of Technology; Guangdong Environmental Monitoring Center;
Guangzhou Institute of Energy Conversion, Chinese Academy of Sciences
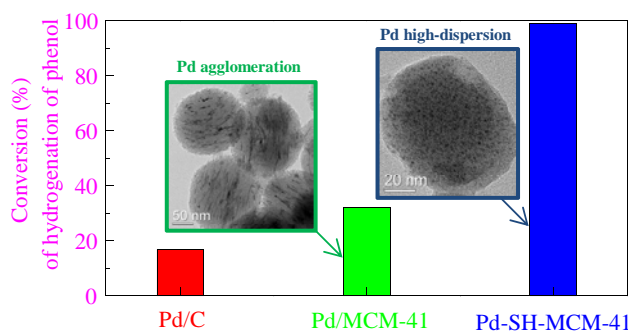
Highly dispersed Pd nanoparticle catalyst on –SH-functionalized mesoporous silica (Pd-SH-MCM-41) was prepared by anchoring interaction between –SH groups and Pd cations. This catalyst showed very high catalytic activity (>99%) for the hydrogenation of phenol.

References

[1] Coti K K, Belowich M E, Liong M, Ambrogio M W, Lau Y A, Khatib H A, Zink J I, Khashab N M, Stoddart J F. *Nanoscale*, 2009, 1: 16

[2] Rosenholm J M, Sahlgren C, Linden M. *Nanoscale*, 2010, 2: 1870

[3] Dodgson I, Griffin K, Barberis G, Pignataro F, Tauszik G. *Chem Ind*, 1989, 11: 830

[4] Xiang Y Z, Ma L, Lu C S, Zhang Q F, Li X N. *Green Chem*, 2008, 10: 939

[5] Li H, Liu J, Xie S H, Qiao M H, Dai W L, Lu Y F, Li H X. *Adv Funct Mater*, 2008, 18: 3235

[6] Li H, Liu J L, Li H X. *Mater Lett*, 2008, 62: 297

[7] Shore S G, Ding E, Park C, Keane M A. *Catal Commun*, 2002, 3: 77

[8] Sikhwivhilu L M, Coville N J, Naresh D, Chary K V R, Vishwanathan V. *Appl Catal A*, 2007, 324: 52

[9] Wang Y, Yao J, Li H R, Su D S, Antonietti M. *J Am Chem Soc*, 2011, 133: 2362

[10] Mahata N, Raghavan K V, Vishwanathan V, Park C, Keane M A. *Phys Chem Chem Phys*, 2001, 3: 2712

[11] Chatterjee M, Kawanami H, Sato M, Chatterjee A, Yokoyama T, Suzuki T. *Adv Synth Catal*, 2009, 351: 1912

[12] Fujita S, Yamada T, Akiyama Y, Cheng H Y, Zhao F Y, Arai M. *J Supercritical Fluids*, 2010, 54: 190

[13] Liu H Z, Jiang T, Han B X, Liang S G, Zhou Y X. *Science*, 2009, 326: 1250

[14] Yang X, Du L, Liao S J, Li Y X, Song H Y. *Catal Commun*, 2012, 17: 29

[15] Du L, Liao S J, Liu Q B, Yang X, Song H Y, Fu Z Y, Ji S. *Int J Hydrogen Energy*, 2009, 34: 3810

[16] Kruk M, Jaroniec M. *Chem Mater*, 2003, 15: 2942

[17] Wang P, Bai S Y, Li B, Yang Q H. *Chin J Catal* (王鹏, 白诗扬, 李博, 杨启华. 催化学报), 2012, 33: 1689

[18] Song M J, Zou C L, Niu G X, Zhao D Y. *Chin J Catal* (宋明娟, 邹成龙, 牛国兴, 赵东元. 催化学报), 2012, 33: 140

[19] Li Y J, Zhou G W, Li C J, Qin D W, Qiao W T, Chu B. *Colloids Surf A*, 2009, 341: 79

[20] Tang S S, Hu Y, Yu D H, Zou B, Jiang L. *Chin J Catal* (唐苏苏, 胡燚, 余定华, 邹彬, 江凌. 催化学报), 2012, 33: 1565

巯基功能化介孔材料高效锚定钯负载型催化剂的制备及其苯酚加氢催化性能

张嘉熙[a]，黄高伟[a]，张 玎[a,b]，何群华[b]，黄 超[a]，杨 旭[c]，宋慧宇[a]，
梁振兴[a]，杜 丽[a,d,*]，廖世军[a,d,#]

[a]华南理工大学化学与化工学院, 广东广州510640
[b]广东省环境监测中心, 广东广州510640
[c]中国科学院广州能源研究所, 中国科学院可再生能源与天然气水合物重点实验室, 广东广州510640
[d]华南理工大学化学与化工学院, 广东省燃料电池技术重点实验室, 广东广州510640

摘要: 以含巯基官能团有机硅烷修饰的介孔材料MCM-41和SBA-15为载体, 采用浸渍-氢气还原法制备了高分散和高活性的负载型Pd催化剂. X射线衍射、N$_2$吸附-脱附和透射电子显微镜表征结果显示, 所制Pd催化剂Pd-SH-MCM-41和Pd-SH-SBA-15具有很好的长程有序结构、分布均匀的孔径、高比表面积及高度分散的Pd颗粒. 苯酚加氢反应结果表明, 以Pd-SH-MCM-41和Pd-SH-SBA-15为催化剂时, 在80 °C, 1.0 MPa反应1 h, 苯酚转化率达99%以上, 环己酮选择性为98%. 它们的催化活性为商业Pd/C催化剂的5倍, Pd/MCM-41和Pd/SBA-15催化剂的3倍. 这可归因于介孔材料表面修饰的巯基官能团对Pd的锚定作用, 避免了Pd颗粒的团聚, 使其高度分散在介孔材料上.
关键词: 介孔氧化硅; 巯基修饰; 钯; 锚定; 负载型催化剂; 苯酚加氢

1. 前言

介孔材料具有规则有序的孔道结构、高的比表面积和大的孔体积以及孔径易调节、表面易功能化等特点, 因而广泛应用于催化、吸附、分离、化学传感器及生物医药等领域. 目前, 有关功能化介孔材料的合成及催化性能是化学、材料、催化领域重要的研究课题之一[1,2].

苯酚是石油化工的副产物和煤焦油提炼的重要馏分, 也是环境有害物质, 如何将其有效转化为有价值的工业原料一直备受关注. 环己酮是工业制备尼龙66的重要原料之一[3], 以苯酚为原料, 经催化加氢可以制取环己酮. 目前, 用于该过程的催化剂包括雷尼镍[4]、Pd基膜/微囊催化剂[5]、非晶合金催化剂[6]、双金属催化剂[7]和负载型催化剂[8,9]等, 但仍然存在催化剂活性较低和反应条件相对苛刻等局限. 例如, 气相苯酚加氢反应常常需要温度在150 °C以上以气化苯酚[10], 而在超临界CO$_2$体系中苯酚加氢催化活性和选择性很高, 但需要10 MPa以上的压力[11,12], 因而限制了催化剂的实际应用. 最近, Liu

等[13]采用路易斯酸-Pd/C组合催化剂, 在温和条件(50 ºC, 1.0 MPa)下实现了苯酚加氢制取环己酮, 选择性大于 99.9%. 这可能是迄今最接近实际应用的苯酚加氢催化剂.

在前期负载型贵金属催化剂催化苯酚加氢反应研究的基础上[14], 本文采用(3-巯基丙基)三甲氧基硅烷对介孔材料MCM-41和SBA-15的表面进行修饰, 然后利用其中的–SH基团对Pd进行锚定, 制备了负载型Pd催化剂, 并考察了催化剂在温和条件下对苯酚加氢反应的催化性能.

2. 实验部分

2.1. 催化剂的制备

2.1.1. MCM-41介孔材料载体的合成

将1.0 g十六烷基三甲基溴化铵(CTAB, Aldrich公司)溶解于480 ml二次水中, 滴加3.5 ml NaOH水溶液(2 mol/L), 在80 ℃磁力搅拌1 h. 将4.5 ml正硅酸乙酯(TEOS, 天津科密欧公司)逐滴加入到上述溶液中, 在80 ℃持续剧烈搅拌, 2 h后停止反应, 待溶液冷却后, 真空抽滤, 用二次水反复洗涤. 将得到的样品置于烘箱中干燥, 研磨成粉末, 于550 ºC焙烧6 h, 即得MCM-41材料.

2.1.2. SBA-15介孔材料载体的合成

将4.0 g P123 ($EO_{20}PO_{70}EO_{20}$, Aldrich公司)溶于126 ml二次水, 再加入20 ml浓HCl (37%), 于35 ℃搅拌2 h以形成稳定胶束. 加入9.2 ml TEOS, 持续搅拌20 h. 转入高压釜中于100 ℃晶化12 h, 冷却后真空抽滤, 用二次水反复洗涤, 烘箱干燥, 研磨成粉末, 于550 ºC焙烧6 h, 即得SBA-15材料.

2.1.3. 巯基(–SH)修饰介孔材料载体的制备

称取100 mg制得的MCM-41或SBA-15分散到10 ml甲苯溶液中, 再加入100 μl (3-巯基丙基)三甲氧基硅烷(Gelest公司), 在80 ºC回流24 h. 将所得固体粉末过滤, 用无水乙醇充分洗涤, 真空干燥后得到固体粉末, 即为–SH修饰的MCM-41和SBA-15, 分别命名为SH-MCM-41和SH-SBA-15.

2.1.4. Pd-SH-MCM-41和Pd-SH-SBA-15催化剂的制备

在小烧杯中加入0.0833 g $PdCl_2$, 2 ml浓盐酸和3 ml H_2O, 超声分散, 再缓慢加入1.0 g SH-MCM-41或SH-SBA-15样品, 浸渍24 h, 然后经二次水反复洗涤, 于70 ℃真空干燥. 最后将样品置于管式电热炉中, 通入H_2 (20 ml/min)于200 ℃还原2 h, 即得Pd催化剂, 分别命名为Pd-SH-MCM-41和Pd-SH-SBA-15. 分别以MCM-41和 SBA-15为载体, 同法制备Pd/MCM-41和Pd/SBA-15催化剂.

2.2. 催化剂的表征

使用日本岛津XD-3A型X射线衍射仪对样品进行X射线衍射(XRD)分析, Cu K_α射线, 电压40 kV, 电流30 mA. 采用美国麦克ASAP 2010型物理分析仪对样品进行N_2吸附-脱附测试, 测样前样品在120 ℃真空脱气预处理24 h. 利用德国Bruker TENSOR 27型傅里叶变换红外光谱(FT-IR)仪研究介孔材料表面基团特性. 透射电镜(TEM)表征在日本JEOL JEM-2010型透射电子显微镜上完成, 加速电压200 kV.

2.3. 催化剂的评价

将1.0 g苯酚、0.2 g Pd催化剂及10 ml二氯甲烷加入到50 ml带聚四氟乙烯内衬及搅拌装置的反应釜中. 反应前, 先用H_2将釜内空气置换3次, 然后充入一定压力的H_2 (99.99%), 升至80 ℃, 再调压到1.0 MPa, 然后开启搅拌, 反应开始计时. 反应1 h后, 将反应产物与催化剂分离, 采用气-质联用色谱(GCMS-QP2010SE, 日本)对反应产物进行定性分析.

3. 结果与讨论

3.1. 载体与催化剂的表征结果

图1是各载体及其负载的Pd催化剂的XRD图. 由图可见, 各样品在小角度范围内均出现一个强的(100)晶面衍射峰和两个较弱的(110)和(200)晶面衍射峰, 说明这些样品均具有很好的长程有序结构. 尽管MCM-41, SH-MCM-41及Pd-SH-MCM-41均出现了典型MCM-41介孔材料的衍射峰(2º–3º), 但经–SH基团修饰和Pd的引入使得样品的(100)晶面衍射峰逐渐向大角度偏移, 这是由于晶面间距变小所致. 同样, SBA-15系列样品也出现相似现象. 另外, Pd/MCM-41和Pd/SBA-15样品中均出现单质Pd的特征衍射峰, 分别对应于Pd(111), (200), (220)和(311)晶面; 同时均在23°附近出现无定形SiO_2的衍射峰[15]. 然而, 在Pd-SH-MCM-41和Pd-SH-SBA-15样品中, 单质Pd的特征衍射峰宽化, 峰形不明显. 这可能是–SH对Pd的锚定使得Pd粒径减小所致.

图2是MCM-41和SBA-15系列样品的N_2等温吸附-脱附曲线及孔径分布曲线. 由图可见, MCM-41, SH-MCM-41和Pd-SH-MCM-41均具有典型的IV型吸附-脱附曲线, 与文献[16]报道的孔径在2–3 nm的吸脱附特征曲线相符合, 没有出现滞后环. SBA-15, SH-SBA-15和Pd-SH-SBA-15样品的吸附-脱附曲线也是IV型, 且在p/p_0

= 0.5–0.8处出现H1型滞后环, 表明其具有介孔结构[17,18]. 各样品的织构性质列于表1. 可以看出, 经–SH修饰的MCM-41和SBA-15仍保持着较高的比表面积, 分别为740和526 m^2/g, 这有利于Pd的高度分散. 负载Pd的SH-MCM-41和SH-SBA-15样品的比表面积虽都有所下降, 但仍高于碳材料负载Pd催化剂(如商业Pd/C催化剂, 250 m^2/g)[14]. 另外, 所有样品均保持了介孔的结构特性, 孔径虽略有减小, 但其分布依然很窄.

图3为MCM-41和SH-MCM-41的FT-IR谱. 由图可见, 各样品均在1089, 797及468 cm^{-1}处出现吸收峰, 可归属为Si–O–Si键的振动[19]; 但SH-MCM-41样品在2939和2835 cm^{-1}处出现可归属为烷基链上C–H键的伸缩振动峰[20]; 在2565 cm^{-1}处出现较弱的S–H键的伸缩振动峰, 进一步说明–SH基团已成功修饰到MCM-41载体上, 为固载Pd提供了位点.

图4是各Pd催化剂样品的TEM照片. 由图可见, Pd-SH-MCM-41样品具有典型MCM-41的介孔孔道结构, 颗粒度约为100 nm. 放大倍数后, 可观测到高度分散的Pd颗粒, 其粒径约为2–3 nm, 分布均匀, 且无团聚现象. Pd/MCM-41和Pd/SBA-15样品表面的Pd颗粒发生了明显的团聚, 粒径较大, 与XRD结果一致. 而Pd-SH-SBA-15样品中Pd颗粒高度分散, 可清晰见到典型SBA-15的介孔孔道结构. 由此可见, –SH的修饰不仅没有破坏介孔材料的孔道结构, 还有利于Pd的高度分散.

3.2. 催化剂的性能

表2是不同催化剂催化苯酚加氢反应结果. 由表可见, 以MCM-41和SBA-15为催化剂时, 反应基本无活性; 商业的Pd/C催化剂上苯酚转化率仅为16.9%; 而以Pd-SH-MCM-41和Pd-SH-SBA-15为催化剂时, 苯酚转化率可达99%以上, 为Pd/C催化剂的5倍多, 环己酮选择性分别为98.1%和97.8%. 由于Pd的团聚使得Pd/MCM-41和Pd/SBA-15催化剂活性明显降低, 苯酚转化率仅为32.2%和31.8%. 实验发现, 当以MCM-41和SBA-15为载体直接负载Pd时, 浸渍24 h后, 上层仍为橙黄色的H_2PdCl_4溶液, 若经大量的二次水反复冲洗过滤, Pd/MCM-41和Pd/SBA-15粉末几乎可被洗至无色. 而用SH-MCM-41和SH-SBA-15负载Pd时, 浸渍24 h后, 上层溶液已变为无色, 所得Pd-SH-MCM-41和Pd-SH-SBA-15粉末为深橙黄色, 经反复冲洗过滤, 滤液仍为无色, 表明Pd已完全负载于载体上. 由此, 反复冲洗后的Pd/MCM-41和Pd/SBA-15的催化活性非常低, 苯酚转化率仅为1.2%和0.9%. 由此可见, MCM-41和SBA-15经–SH修饰后再负载Pd, 所得催化剂具有较高活性.

4. 结论

利用(3-巯基丙基)三甲氧基硅烷对介孔材料MCM-41和SBA-15表面进行修饰, 使之含有–SH活性基团, 可将Pd锚定于其上, 从而制得高度分散的Pd催化剂. 结果表明, –SH与Pd的引入并未破坏介孔材料, 介孔材料仍然保持分布均匀的孔道结构及较高的比表面积. 在苯酚加氢反应中, Pd-SH-MCM-41和Pd-SH-SBA-15催化剂活性分别是商业催化剂(Pd/C)和传统方法制备的Pd/MCM-41和Pd/SBA-15催化剂的5倍和3倍以上. 由此可见, 利用–SH活性基团与Pd的锚定作用可制备出具有高度分散和高催化活性的Pd催化剂, 可为其它负载型金属催化剂提供一个新的制备方法.